Evaluation of Methods for Predicting Complex Aircraft Flowfields

A. Cenko*
U. S. Naval Air Development Center, Warminster, Pennsylvania
and
F. Tessitore†
Grumman Aerospace Corporation, Bethpage, New York

Reliable methods for predicting external aircraft flowfields are required for airframe/engine and aircraft/store integrations, as well as for predicting store trajectories. Several analytical techniques exist that can predict the flowfield about complete aircraft configurations. Three of these – the PAN AIR panel method, the Boppe transonic small disturbance code, and the influence function method (IFM) technique – are examined in this paper. All three methods have certain advantages and disadvantages. The PAN AIR method has the greatest geometric flexibility, but only gives consistently good results at subsonic speeds and lacks an integrated boundary layer calculation. The Boppe code gives a better prediction of wing-induced flowfield effects at all Mach numbers but cannot properly account for body-induced effects. The IFM method has the best ability to predict aircraft flowfield effects but requires store grid force and moment data in a horizontal traverse to make the flowfield predictions.

Introduction

ONE attempt to predict complex aircraft flowfields was reported in Refs. 1 and 2. Although the PAN AIR code[3] exhibited good correlation with experimental data for the subsonic cases, two drawbacks were evident at supersonic speeds. The code usually overpredicted the effects of the inlet shock, and its location had to be shifted to account for the discrepancy between Mach wave and shock wave locations (Fig. 1).

Reference 4 described the ability of the Boppe[6] code to predict inlet flowfields for generalized forebodies. The code showed qualitative agreement with the test data, but the quantitative correlations were unimpressive, particularly for the sidewash comparisons.

The influence function method (IFM)[6] technique was developed primarily to predict store forces and moments induced by an aircraft flowfield. The procedure is based on determmining how the aircraft flow disturbances affect the store forces and moments. It has been shown[7,8] that, given store loads in a horizontal traverse under the aircraft, the technique can accurately predict the aircraft flowfield at that traverse. As may be seen in Figs. 2 and 3, the upwash and sidewash are accurately predicted 2.3 ft below and 1.5 ft to the side of the F-15 pylon at $M = 1.2$. The purpose of this paper is to evaluate the relative merits of these three methods.

Description of the Computer Codes

PAN AIR Panel Method

PAN AIR is a higher-order panel method developed for the solution of linearized potential flows about arbitrary configurations. A more complete description of the method is available in Refs. 9 and 10.

Principal features that distinguish the technique from lower-order panel methods are the incorporation of logically independent networks, the use of higher-order singularities, and the possibility of various boundary condition specifications.

The configuration surface is represented by a distribution of source and doublet singularities. The singularities may be placed on the actual configuration surface, or may be used to represent components (such as thin wings) in linearized fashion by representing both upper and lower surfaces as a thin sheet along the camber line.

The configuration surface is divided into networks. A network is defined as a smooth portion of the configuration that is subsequently divided into panels, each panel representing some source and doublet distribution. Both a linear source and quadratic doublet distribution over the panels are defined in terms of the values of the singularities at the centers of each panel and neighboring panels by a system of spline-type polynomials. Boundary conditions are applied at discrete points associated with each network. The required integrals are evaluated in closed form, and the resulting set of linear equations is solved separately for the required singularity strength parameters for each network.

The PAN AIR program gives the user various options for specifying the boundary conditions. Several investigators[11,12]

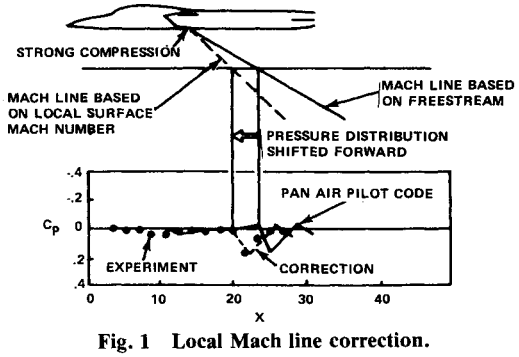

Fig. 1 Local Mach line correction.

Presented as Paper 86-0396 at the AIAA 24th Aerospace Sciences Meeting, Reno, NV, Jan. 6–9, 1986; received March 31, 1987; revision received Jan. 11, 1988.

*Aerospace Engineer, Aerodynamics Branch. Member AIAA.
†Project Manager, Guided Weapon Systems. Member AIAA.

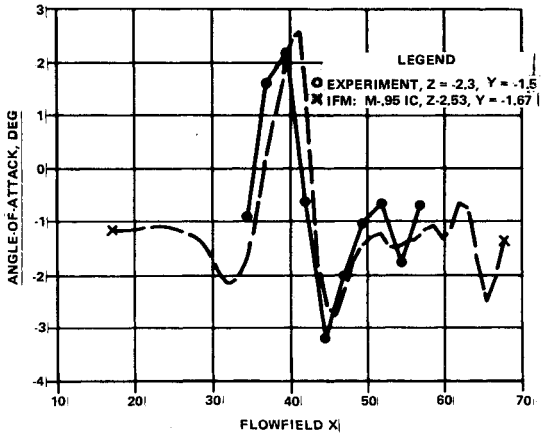

Fig. 2 F-15 pitch flowfield prediction from PWW store, $M = 1.2$.

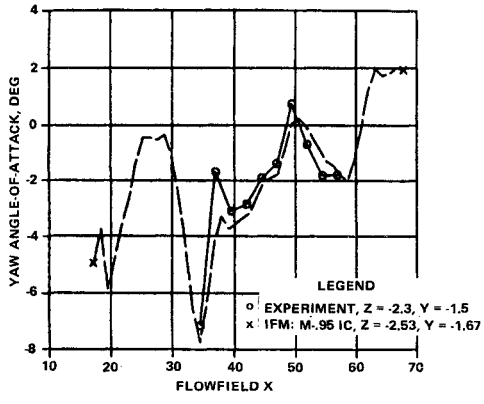

Fig. 3 F-15 yaw flowfield prediction from PWW store, $M = 1.2$.

have commented on the need to use velocity boundary conditions at supersonic speeds. Although at subcritical Mach numbers mass flux boundary conditions give good results, for the sake of consistency all the results in this paper are based on the velocity boundary condition formulation.

Since the pilot code does not have the streamline tracing capability, a network was prescribed to have only source panels of zero strength in order to calculate the off-body velocities. This network was thus eliminated from the calculation and only used to interrogate the flowfield at its position.

Boppe Code

The Boppe code could be classified as an extended transonic small disturbance formulation. The differential equation employed is

$$\left[1 - M_\infty^2 - (\gamma+1)M_\infty^2\zeta_x - \frac{\gamma+1}{2}M_\infty^2\zeta_x^2\right]\zeta_{xx} - 2M_\infty^2\zeta_y\zeta_{xy} + [1-(\gamma-1)M_\infty^2\zeta_x]\zeta_{yy} + \zeta_{zz} = 0 \quad (1)$$

This differs from the classic small disturbance formulation by the addition of three terms. The crossflow terms $\zeta_x\zeta_{yy}$ and $\zeta_y\zeta_{xy}$ were added to provide the capability of capturing shock waves with considerable sweep relative to the onset flow, whereas the higher term $\zeta_x{}^2\zeta_{xx}$ was included to provide a better approximation to the full potential equation critical velocity.

The finite-difference approximations are described in detail in Ref. 5. It is worth noting, nowever, that this code pioneered the concept of the imbedded grid approach. The program uses three different grid systems for the analysis of wing-body

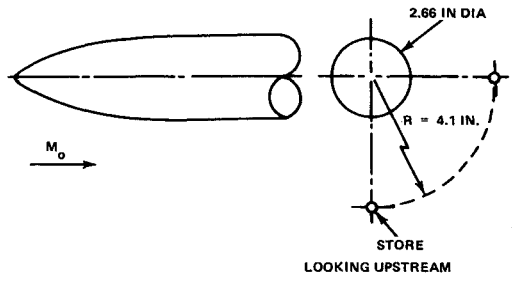

Fig. 4 Ogive-cylinder flowfield gnerator.

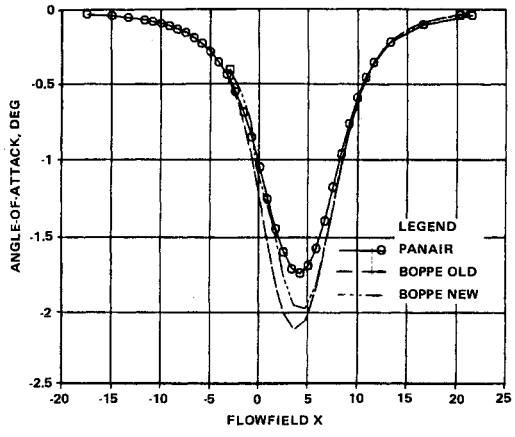

Fig. 5 Prediction of calibrator flowfield: PWW predicted flowfield at $M = 0.6$, $Z/D = 1.5$.

configurations. A fine mesh surrounds the wing, another encompasses the body, and a global crude grid fills the entire computational region. This approach allows the modeling of fine geometric features of both the wing and body at a considerable reduction in computer costs.

Boundary conditions are imposed in the plane of the wing and on a constant cross-sectional shell that approximates the true body shape. More than a decade of comparisons with experimental results have demonstrated the ability of this approach to predict fuselage effects accurately in wing-body calculations.

IFM Technique

The IFM technique is a three-step process that alternatively employs the following equations:

$$C_N - C_{N_o} = \sum_{i=1}^{N} A_i\alpha_i \quad (2a)$$

$$C_m - C_{m_o} = \sum_{i=1}^{N} B_i\alpha_i \quad (2b)$$

These equations represent the relationship between the forces and moments acting on a store, and the interaction of the local flow angle on each store with the store normal force and pitching moment influence coefficients A_i and B_i, respectively. Note that although these equations are linear in form, they do not represent linearized aerodynamic effects. The equations are actually analogous to regression equations where the nonlinear effects are included in the influence coefficient terms as well as a general nonlinear angularity represented by α_i. The formulation for the sidewash as a function of side force and yawing moment is identical.

The first step of the IFM process is the determination of the store's influence coefficients. Loads data for a store along an axial traverse of N positions in a known flowfield provide a set of N equations which can be solved for the N unknown influence coefficients A_i and B_i by matrix inversion. In the

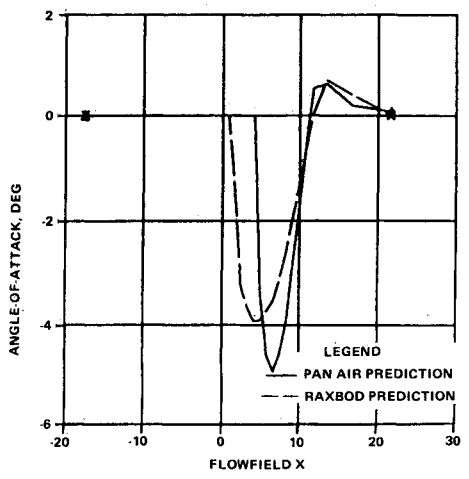

Fig. 6 Prediction of calibrator flowfield at $M = 1.2$, $Z = 6.89$.

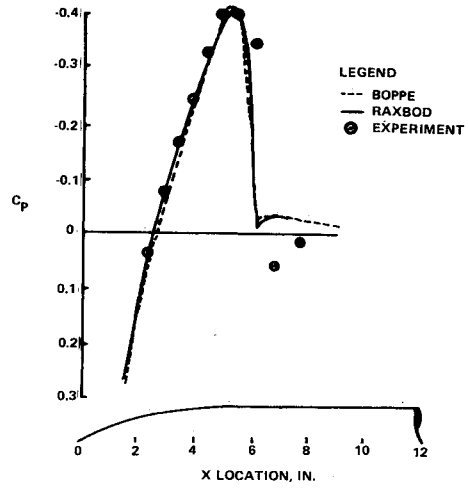

Fig. 7 $M = 0.95$ calibrator body pressures.

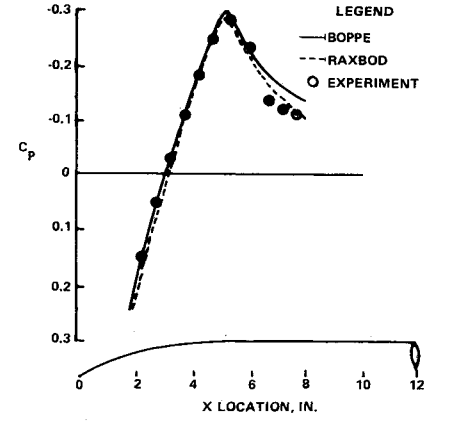

Fig. 8 $M = 1.05$ calibrator body pressures.

second step, experimental C_N and C_m data from an axial traverse through an aircraft flowfield for a calibrated store may be used to determine the unknown flowfield through which the store has passed. The final step of the process combines the flowfield calculated in the second step with influence coefficients for another calibrated store to calculate that store's forces and moments within an aircraft flowfield.

Although the second step in the IFM process was not developed for the purpose of calculating aircraft flowfields,

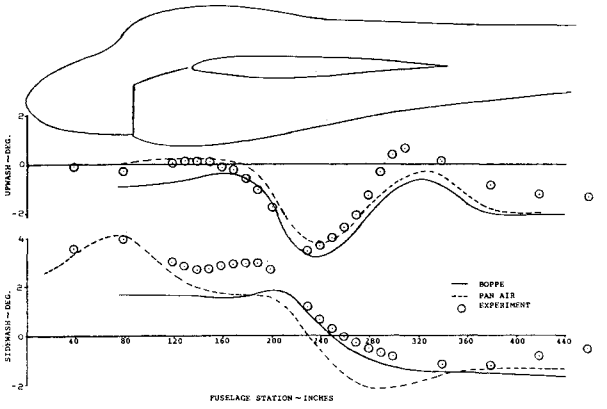

Fig. 9 A-6E flowfield: $M = 0.6$, $BL = 95$, $WL = 65$.

extensive correlations with experimental aircraft flowfield data have demonstrated the capability of IFM to predict complex aircraft flowfields accurately at all Mach numbers to within one store diameter of the aircraft surface. (It appears[13] that, for traverses closer than one diameter to the aircraft surface, mutual interference between the store and aircraft may violate the basic assumption in [Eqs. (2)] that the store has no influence on the flowfield produced by the aircraft). Furthermore, since the calibration process can be performed analytically,[7,14,15] the IFM process can now be used with any experimental store traverse data in the axial direction to predict that aircraft's flowfield along the traverse.

Axisymmetric Body Flowfield

The first case considered was the flowfield generated by an ogive-cylinder body at zero angle-of-attack at a distance of 1.5 diam from the body surface (Fig. 4). Comparisons at $M = 0.6$ of the flowfields predicted by the Boppe and PAN AIR codes are shown in Fig. 5. Numerous comparisons with test data and exact linear theory have established the validity of the PAN AIR code at subcritical Mach numbers for simple body shapes. The overprediction of the maximum flowfield disturbance exhibited by the old Boppe code is attributed to the code's use of a constant cross section to represent the body. Furthermore, the code sets the X component of the perturbation velocity to zero when satisfying the body boundary condition.[5] When this term ζ_x was included in the body boundary conditions,

$$N_x(1 + \zeta_x) + N_y\zeta_y + N_z\zeta_z = 0 \qquad (3)$$

the prediction was somewhat improved (Fig. 5, new Boppe).

It has been previously observed[15] that the Boppe code cannot accurately predict flowfields for bodies of rapidly varying cross sections unless the body grid is modified to conform to the true body shape.

Note that the PAN AIR code at supersonic speeds overpredicts both the magnitude and location of the maximum flowfield disturbance when compared to the RAXBOD[16] code (Fig. 6). Although the RAXBOD code provides a solution to the full potential equation, its utility is somewhat limited since it is only applicable to axisymmetric or two-dimensional shapes.

Although the Boppe code did not accurately predict the calibrator body flowfield, its surface pressure predictions were in excellent agreement with the test data, as well as the RAXBOD code, at $M = 0.95$ and 1.05 (Figs. 7 and 8).

A-6E Flowfield Predictions

David Taylor Naval Ship Research and Developmnet Center (DTNSRDC) flowfield test data were available for the

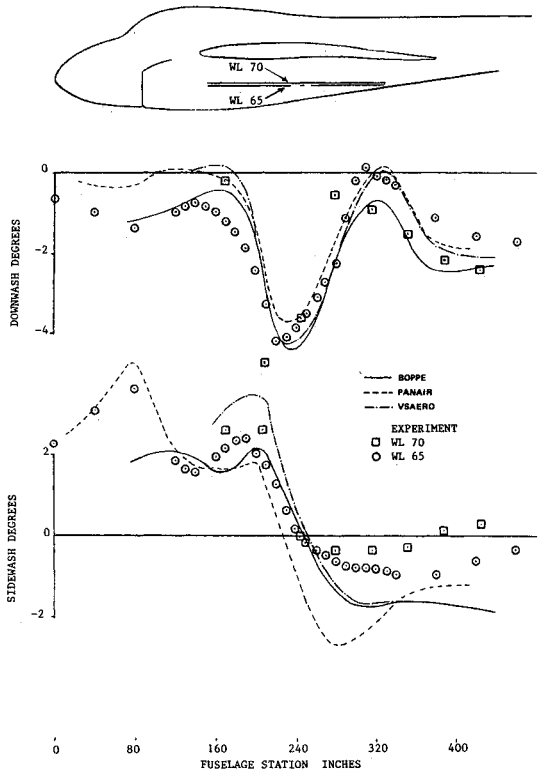

Fig. 10 A-6E flowfield: $M = 0.85$, $BL = 95$, $WL = 65,70$.

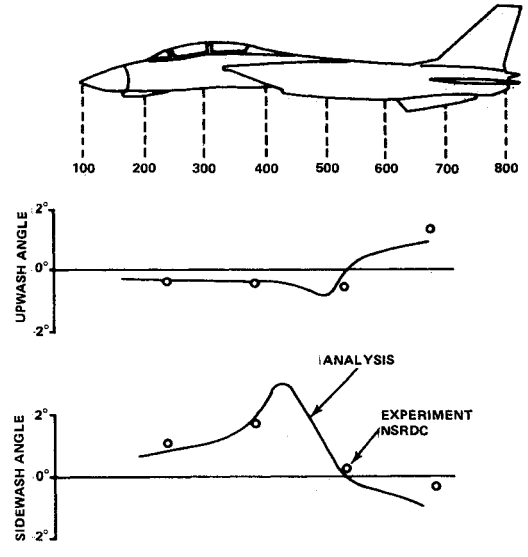

Fig. 11 F-14A flowfield angularity correlation: $M = 0.8$, $\Lambda = 68$.

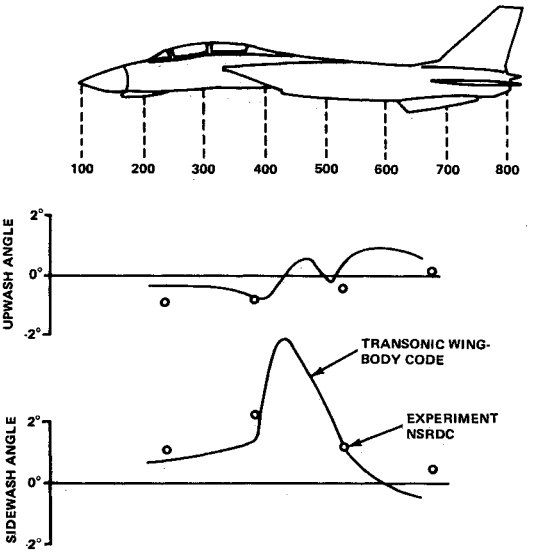

Fig. 12 F-14A flowfield angularity correlation: $M = 1.2$, $\Lambda = 68$.

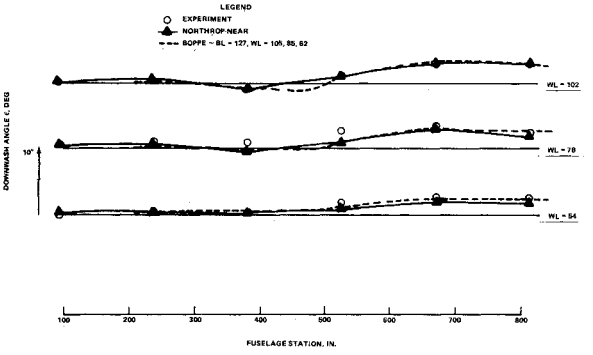

Fig. 13 F-14 pitch flowfield: $M = 0.6$, $BL = 124.5$.

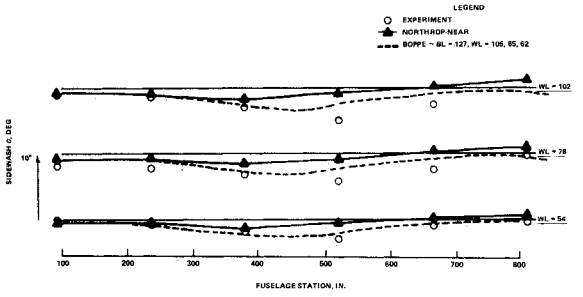

Fig. 14 F-14 yaw flowfield: $M = 0.6$, $BL = 124.5$.

A-6E aircraft at $M = 0.6$ at the inboard wing pylon store carriage location. Boppe and PAN AIR comparisons with test data are shown in Fig. 9. Both codes agree with the test data for the wing induced downwash up to the wing trailing edge at fuselage station 349. Boundary layer separation might account for the discrepancy aft of this point. The sidewash effects are not well predicted by either code. The Boppe code misses the outboard flowfield generated by the nacelle inlet, probably because the constant body cross-section model is most in error at this point. The PAN AIR program considerably overpredicts the inboard flowfield produced by the body of the nacelle. This might be attributed to the PAN AIR model, which, due to the pilot code's limitation on the total number of panels, blended the aft end of the nacelle into the fuselage. The production version of the code, which allows the user twice as many panels, should give better results if the nacelle exhaust is properly represented.

DTNSRDC flowfield test data were available at $M = 0.85$ and $BL = 95$, at two different waterlines, $WL = 65$ and 70. Since the PAN AIR code predicted only minor variations in the flow angularities between the two waterline locations (Fig. 10), Boppe and VSAERO[17] predictions are shown only for $WL = 70$. All three codes predict the downwash reasonably well. At this Mach number, the transonic flow regions were predicted by all three codes. Since the PAN AIR and VSAERO codes are in close agreement with the test data, transonic effects on the wing flowfield may be small at the pylon carriage location.

None of the three codes are in good agreement with the sidewash data, particularly at the aft end of the nacelle. This

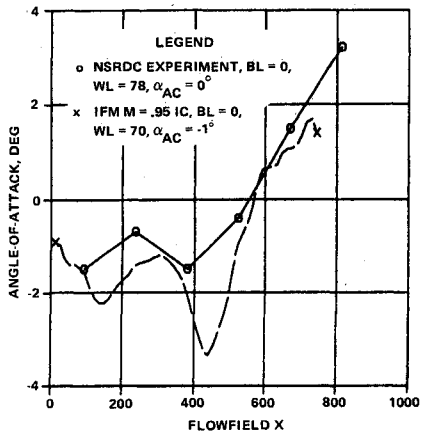

Fig. 15 F-14 pitch flowfield prediction from AMRAAM store, $M = 0.8$.

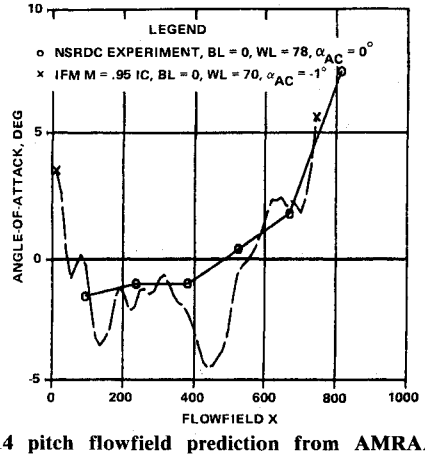

Fig. 16 F-14 pitch flowfield prediction from AMRAAM store, $M = 1.05$.

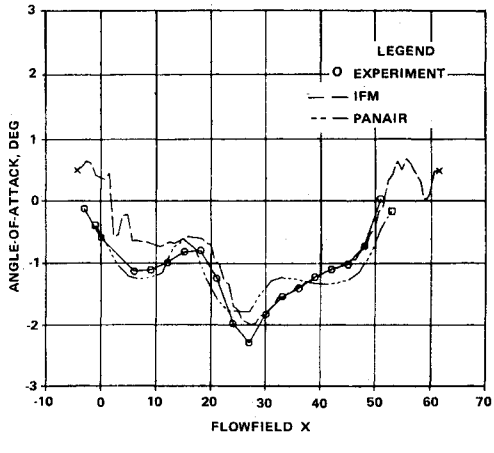

Fig. 17 AWECS pitch flowfield prediction from ogive cylinder store, $M = 0.6$, $Z = -6.08$, $Y = 0$.

might be due to flow separation effects, which seem to be indicated by the $WL = 70$ data.

F-14 Flowfield

Experimental flowfield data were available at $BL = 124.5$ and $WL = 102$. Comparisons between the Boppe flowfield predictions and the test data are shown in Fig. 11 at $M = 0.8$, and Fig. 12 at $M = 1.2$. The Boppe code not only accurately predicts the downwash and sidewash, but also demonstrates

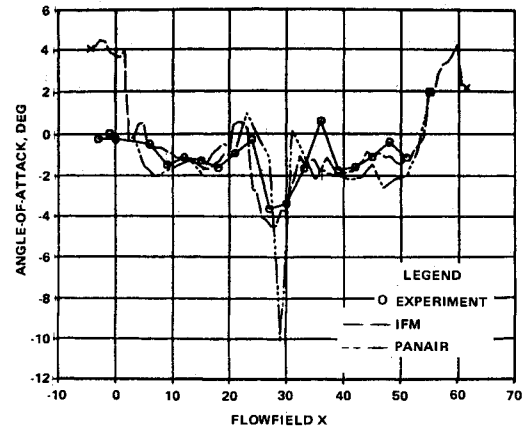

Fig. 18 AWECS pitch flowfield prediction from ogive cylinder store, $M = 1.2$, $Z = -6.08$, $Y = 0$.

that the experimental flowfield was too sparse to determine the nacelle inlet effect properly. Comparisons between the Boppe code and the Northrop-NEAR predictions[18] at three waterlines (102, 78, and 54 in.) with test data are shown in Figs. 13 and 14. The Boppe sidewash predictions are clearly superior, while the downwash predicitons are the same for both codes.

Since Advanced Medium Range Air to Air Missile (AMRAAM) store traverse data were also available for the F-14 aircraft, IFM predictions of the F-14 flowfield are shown in Figs. 15 and 16 for $M = 0.8$ and 1.05. The AMRAAM test was conducted with full inlet spillage, which accounts for the disagreement between the predictions and flowfield test data at fuselage station 400. This indicates how IFM predictions can be used to evaluate the effects of configuration changes between wind tunnel tests.

AWECS Flowfields

Since ogive-cylinder traverse data were available for the AWECS configuration shown in Fig. 1, the IFM code was used to predict the flowfields at $M = 0.6$ and 1.2. These predictions are compared with those of the PAN AIR code and experimental probe flowfield test data in Figs. 17 and 18. Note that while PAN AIR provides good flowfield predictions at $M = 0.6$, it substantially overpredicts the effect of the inlet shock at $M = 1.2$. The IFM code provides good flowfield predictions at both Mach numbers.

Conclusions

All three methods examined for flowfield predictions have certain advantages and disadvantages. The PAN AIR code provides the greatest geometric flexibility, but gives consistently good results only at subsonic speeds. The code can be used to provide good estimates of the effects of small configuration changes on known flowfields at all Mach numbers.

The Boppe code exhibited the best correlation at all Mach numbers for wing induced flowfield effects. Until the code is modified to accept a conformal body grid, it cannot be expected to provide reliable information in regions of rapidly changing body curvature.

The IFM technique has shown the best ability of predicting aircraft flowfields on the basis of store traverse test data. Since the code requires experimental data to make flowfield predictions, its utility is somewhat limited.

Acknowledgments

The authors wish to express their appreciation to C. Boppe, W. Gatto, J. Guarracino, B. Rosen, and A. Zigomalas of Grumman Aerospace Corporation, without whose aid this paper would not have been possible.

References

[1]Cenko, A. and Tinoco, E.N., "PAN AIR – Weapons, Carriage and Separation," Air Force Flight Dynamics Labs-TR-79-3142, Dec. 1979.

[2]Cenko, A., Tinoco, E.N., Dyer, R.D., and DeJongh, J., "PAN AIR Applications to Weapons, Carriage and Separation," *Journal of Aircraft*, Vol. 18, Feb. 1981, pp. 129–134.

[3]Magnus, A.E. and Epton, M.A., "PAN AIR – A Computer Program for Predicting Subsonic or Supersonic Linear Potential Flows about Arbitrary Configurations Using a Higher Order Panel Method," NASA-CR-3251, Vol. 1, 1980.

[4]Yaros, S.F., "Evaluation of Two Analytical Methods for Prediction of Inlet Flowfields in the Vicinity of Generalized Forebodies," AIAA Paper 82-0959, June 1982.

[5]Boppe, C.W., "Transonic Flowfield Analysis for Wing-Fuselage Configurations," NASA CR-3242, May 1980.

[6]Cenko, A., Tessitore, F., and Meyer, R., "Prediction of Aerodynamic Characteristics for Weapon Separation," AFWAL-TR-82-3025, April 1982.

[7]Cenko, A., Tessitore, F., and Meyer R., "Influence Function Prediction of Store Trajectories," AFWAL-TR-84-3057, Aug. 1984.

[8]Cenko, A., Tessitore, F., and Meyer, R., "IFM – A New Approach to Predicting Store Loads in Proximity to Fighter Aircraft and Their Influence on the Subsequent Trajectories," AGARD CP-12, Oct. 1985.

[9]Tinoco, E.N., Johnson, F.T., and Freeman, L.M., "The Application of a Higher Order Panel Method to Realistic Supersonic Configurations," AIAA Paper 79-0174, Jan. 1979.

[10]Carmichael, R.L. and Erickson, L.L. "PAN AIR – A Higher Order Panel Method for Predicting Subsonic or Supersonic Linear Potential Flows about Arbitrary Configurations," AIAA Paper 81-1255, June 1981.

[11]Cenko, A., "PAN AIR Applications to Complex Configurations," *Journal of Aircraft*, Vol. 20, Oct. 1983, pp. 887–892.

[12]Melnik, R. and Mason, W., "Mass Flux Boundary Conditions in Linear Theory," *AIAA Journal*, Vol. 22, Nov. 1984, pp. 1691–1692.

[13]Cenko, A., Tinoco, E.N., and Tustaniwski, J., "PAN AIR Applications to Mutual Interference Effects," *Journal of Aircraft*, Vol. 21, Oct. 1984, pp. 803–808.

[14]Keen, K.S., "Economic Influence Function Calibrations Using the Distributed Loads Code, *Journal of Aircraft*, Vol. 22, Jan. 1985, pp. 85–87.

[15]Rosen, B., "Body Flowfield Simulation and Force/Moment Prediction at Transonic Speeds," AIAA Paper 85-0423, Jan. 1985.

[16]Grossman, R. and Melnik, R., "The Numerical Computation of Transonic Flow Over Afterbodies Including the Effect of Jet Plume and Viscous Interactions," AIAA Paper 75-0062, Jan. 1975.

[17]Maskew, B., "Prediction of Subsonic Aerodynamic Characteristics – A Case for Low Order Panel Methods," AIAA Paper 81-0252, Jan. 1981.

[18]Nadir, S., "The Northrop/NEAR Subsonic Store Separation Method," Sixth Biennial Aircraft/Stores Compatability Symposium, White Oak, MD, Paper 12, Oct. 1982.